# Material Properties in Thermal-stress Analysis

**I. Miskioglu*, C. P. Burger**, *Iowa State University and* J. Gryzagoridis***, *University of Cape Town***

*With simple techniques and not too-costly laboratory equipment, the significant material properties in modeling transient thermal stresses by photothermoelasticity are evaluated. The results are presented for a room-temperature-cured epoxy, a hot-cured epoxy and a polycarbonate. The materials tested are also evaluated on their applicability to a transient-thermal-stress analysis.*

### Nomenclature

$A$ = area
$a$ = coefficient of thermal expansion
$\beta$ = thermal diffusivity, $k/\varrho C_p$
$C_p$ = specific heat
$E$ = Young's modulus
$\epsilon$ = strain
$f_\sigma$ = photoelastic-fringe coefficient
$h$ = beam thickness or plate thickness
$I$ = area moment of inertia
$k$ = thermal conductivity
$\lambda$ = wavelength of light
$\ell$ = length
$\nu$ = Poisson's ratio
$M$ = bending moment
$m$ = mass
$N$ = photoelastic-fringe number
$P$ = load
$Q_t$ = figure of merit, $Ea/f_\sigma$
$R$ = electrical resistance
$\varrho$ = mass density
$\sigma$ = principal stress
$\Delta T$ = temperature difference
$V$ = voltage
$y$ = distance from neutral axis of a beam

### Introduction

Experimenters in thermal-stress analysis are very often hampered in their work because the properties of the resins, epoxies, etc., used in their models are not fully known. In certain cases where some properties are published by the manufacturers, uncertainty exists regarding the variation of these properties with temperature.

Der Hovanesian and Kowalski[1] showed that the thermal diffusivity, $\beta = k/\varrho C_p$, is the governing parameter for heat flow within a solid in transient conditions. Hence, the properties of the thermal conductivity $k$, specific heat $C_p$, and density $\varrho$, together with other properties such as the coefficient of thermal expansion $a$, Young's modulus $E$, Poisson's ratio $\nu$, and the photoelastic-fringe coefficient $f_\sigma$, all play a role when the time of occurrence of certain stress states in a thermal-stress model is scaled with respect to a prototype.

It is common practice in photoelasticity to employ a figure of merit, $Q$, to compare different model materials. For photothermoelasticity, the figure of merit is of the form $Q_t = Ea/f_\sigma$. The important heat-transfer parameter (thermal diffusivity) should also be used in conjunction with the figure of merit in the evaluation of model materials for transient-thermal-stress analysis.

Burger[2,3] reported values for a hot-cured epoxy, Araldite B[1] with Hardener 901, and discussed some of the significance of the combined variables with respect to steady-state and transient-temperature fields. Tsuji and Oda[4] reported the optical and physical properties of epoxy resin Araldite B, and Marloff[5] discussed the properties for an aluminum-filled epoxy, Model Tech FRL-20.

This paper demonstrates that, with fairly simple techniques and relatively standard laboratory equipment, the properties of many modeling materials can be evaluated. In what follows, the procedures used to find all of the significant properties over a wide-working range of temperatures are described and exemplified on three model materials. Results are presentesd for a room-temperature-cured epoxy Araldite 502 with Hardener 951; a hot-cured epoxy, Epon 828 with phthalic anhydride hardener; and a polycarbonate, PSM-1.[2]

### Experimental Apparatus and Procedure

*Young's Modulus and Poisson's Radio*

The two elastic constants, Young's modulus and Poisson's ratio, were determined by using a tensile specimen as shown in Fig. 1. The specimen with longitudinal and transverse strain

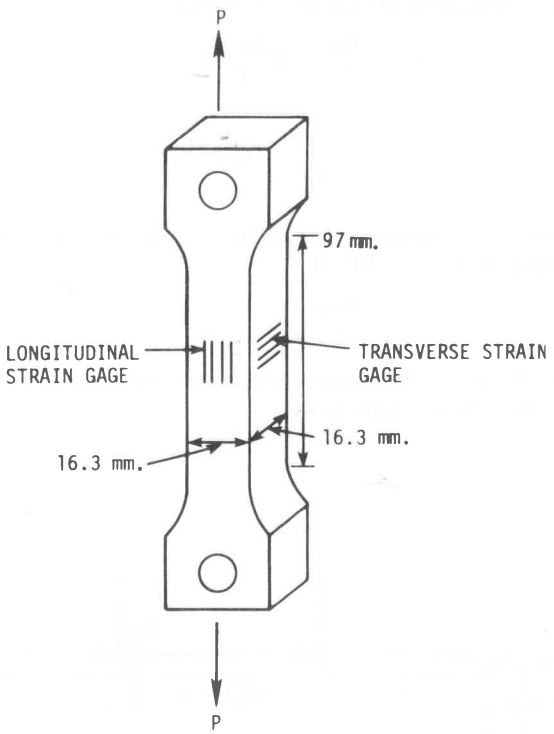


**Figure 1 – Tension-test specimen for determination of $E$ and $\upsilon$**

*Research Assistant, Department of Engineering Science and Mechanics
**Professor
***Professor, Departement of Mechanical Engineering
Reprinted from Experimental Mechanics, August 1981

1. Mention of commercial products or trade names does not constitute an endorsement by the Engineering Research Institute of Iowa State University.
2. PSM-1 is a product of Photolastic, Inc., Raleigh, NC 27611.

gages mounted on it (such as to eliminate bending strains) was placed in an environmental chamber capable of maintaining stable temperatures to within 0.3 °C for the range of −70 °C to 170 °C. The gages were also compensated for temperature. The specimen was cooled to −40 °C and allowed to stabilize. The 'no load' strains in the longitudinal and transverse directions were then read. Load was applied in the axial direction and the 'load on' strains were recorded. Subsequently, a new temperature was established and new values for the 'no load' and 'load on' conditions were obtained. This procedure was repeated at approximately 10 °C intervals from −40 °C to 70 °C.

Young's modulus was evaluated for each temperature by using the one-dimensional Hooke's Law as

$$E = \frac{P/A}{\epsilon_l} \tag{1}$$

where $\epsilon_l = (\epsilon_{load} - \epsilon_{no\ load})_{longitudinal}$.

Poisson's ratio was determined for each temperature setting by the ratio

$$\nu = \frac{\epsilon_t}{\epsilon_l} \tag{2}$$

where $\epsilon_t = (\epsilon_{load} - \epsilon_{no\ load})_{transverse}$.

For the above procedure, 120-Ω gages were used. Local reinforcement was checked using an optical extensometer and was found to be negligible. To reduce the effect of creep of the material, care was taken to keep the loading time about 10 s when data were being recorded. Also, a low bridge current of 10 mA was used to minimize local-heating effects.

*Photoelastic-fringe Coefficient*

In order to determine the fringe coefficient of the material, a beam in pure bending was used as depicted in Fig. 2. Light-field photographs of the fringes were taken in the midsection of the beams. In this region, the fringes were parallel and symmetric with respect to the neutral axis, x. Using

$$\sigma = \frac{My}{I} = \left(\frac{Pa/2}{I}\right)y \tag{3}$$

and

$$(\sigma_1 - \sigma_2) = \frac{Nf_\sigma}{h} \tag{4}$$

since $\sigma_2 = 0$ for pure bending and $\sigma_1 = \sigma$ given by eq (3), then substituting for $I = hb^3/12$

$$f_\sigma = \frac{6Pa}{b^2} \frac{1}{N_u + N_L} \tag{5}$$

where $N_u$, $N_L$ = extrapolated fringe order at upper and lower beam boundaries, respectively.

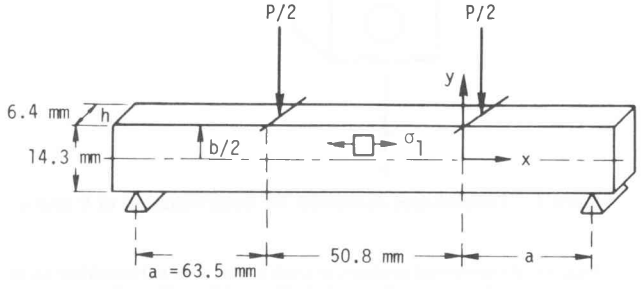


**Figure 2 – Bending specimen for determination of $f_\sigma$**

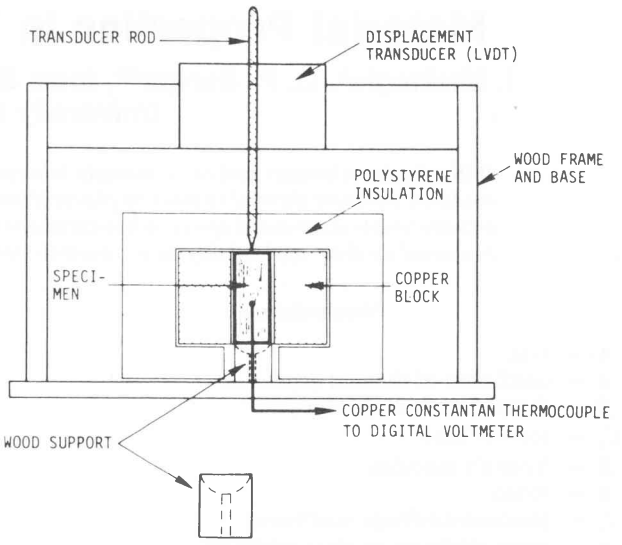


**Figure 3 – Diagrammatic of apparatus for finding $\alpha$**

The light source was a helium-neon laser ($\lambda = 632.8$ nm). Subsequently, the beam was placed in the environmental chamber described in the previous section and the photographs of the fringes at tempertures ranging from −40 °C to 70 °C were obtained.

Again the procedure required the loading time to be short to avoid creep of the material. The loading time for this test was also about 10 s.

*Coefficient of Thermal Expansion*

Cylindrical specimens of length 12.7 mm (0.5 in.) and 3.18 mm (0.125 in.) in diameter were prepared. A copper-constantan thermocouple was embedded in the specimen and it was placed in a simple apparatus as shown in Fig. 3. The high specific heat of the copper block ensured a large heat sink/source and even temperatures along the length of the specimen. The wood support was chosen because of its very low thermal conductivity and low coefficient of thermal expansion. Conduction was further reduced by hollowing out the top of the wood support so that the area of contact with the specimen was small.

The test was performed as follows. The hollow cylindrical copper block was heated in the oven up to 120 °C and then placed over the specimen. The specimen was heated by radiation and its temperature was monitored on a digital voltmeter. When the highest temperature was obtained, the copper block was removed and the transducer rod was placed in contact with the upper surface of the specimen. As it cooled down to ambient conditions, the specimen contracted, thus displacing the transducer rod relative to the tansducer core. Simultaneous readings were obtained of temperature and transducer output. The same procedure was repeated by cooling the copper block to −40 °C in the environmental chamber. Thus, a set of displacement vs. temperature data was obtained for a temperature range of −25 °C to 60 °C. The coefficient of thermal expansion is then evaluated from

$$\alpha = \frac{1}{\ell_o} \frac{d\ell}{dT} \tag{6}$$

where $\ell_o$ is the initial length of the specimen.

The sources of error were in positioning the specimen on the wooden support and in the heat lost through the transducer rod and the thermocouple wires.

Heat lost through the transducer rod was negligible because the transducer rod offered minimum contact area (sharp point) with the upper surface of the specimen.

To decrease the thermocouple conduction error, the portion of the thermocouple wires that were not embedded in the specimen were insulated. This reduced the heat exchange between the thermocouple wires and the ambient. This heat exchange leads to higher temperature readings when the specimen temperature is below ambient and to lower temperature readings when the specimen temperature is above ambient temperature. As a check measure, tests were performed using acrylic, copper and aluminum specimens. The values obtained were $8.5 \times 10^{-5}$ °C for acrylic, $1.74 \times 10^{-5}$ °C for copper and $2.41 \times 10^{-5}$ °C$^{-1}$ for aluminum. These results compare within 6 per cent of the published values in standard handbooks.

*Specific Heat*

A rectangular piece of material was refrigerated to approximately −70 °C (temperature was indicated by a thermocouple embedded at its center). The specimen was placed into a thermoflask containing a known mass of water at room temperature and, after a short period of time, equilibrium was established (water and specimen temperatures were identical). A heat balance yielded

$$(mC_p\Delta T)_{water} = (mC_p\Delta T)_{specimen} + \text{loss} \qquad (7)$$

The loss is the heat transfer between the water and the inner glass container of the thermoflask. If the quantity $(mC_p\Delta T)_{water}$ is plotted as the ordinate and $(m\Delta T)_{specimen}$ is plotted as the abscissa, then from eq (7) a straight line should be obtained with a slope of $C_p$ (if $C_p$ is a constant) and intercept 'loss'. Thus, $C_p$ was determined from the slope of the $(mC_p\Delta T)_{water}$ vs. $(m\Delta T)_{specimen}$ curve over the range of temperatures where it was a constant. Data were taken for the temperature range of −70 °C to 70 °C.

*Thermal Conductivity*

The thermal conductivity of the material was determined using a guarded hot plate.[6] The plate measured 203 mm × 203 mm (8 in. × 8 in.) and was constructed according to ASTM standards (Fig. 4). The guarded hot plate is widely used for determining the conductivity of nonmetals, i.e., solids of rather low thermal conductivity.

The apparatus consists of a main heater which supplies the heat to the specimen. Surrounding this heater is the 'guard heater' which has its temperature maintained at that of the main heat. This prevents heat transfer sideways through the material whose thermal conductivity is to be determined. Two plates of the specimen material, each equipped with copper-constantan thermocouples on their outer and inner surfaces sandwiched the guarded plate. The thermocouples measure the temperature drop, $\Delta t$, for the one-dimensional heat flow through the thickness of the specimens. The heat flow through the central square portion of the specimens can be found from the power input $V^2/R$ to the main heater element. In order to hold the boundary conditions steady, the whole assembly is placed in an environmental chamber for the duration of the test. Tests were conducted from −60°C to 60 °C.

The test procedure was as follows. Once steady-state conditions were established (that is, the thermocouples monitoring the main heater's and the guard heater's surfaces indicated identical and steady readings), the power input to the main heater as well as the temperature of the two surfaces in contact with the main heater were noted. At steady-state conditions the heat transfer through the specimen equals the amount of electrical power to the heater; hence, the thermal conductivity can be evaluated from

$$k = \frac{V^2}{R}\frac{h}{A(\Delta T)} \qquad (8)$$

where $h$ = the thickness of the specimen plates, and $A$ is the central test area.

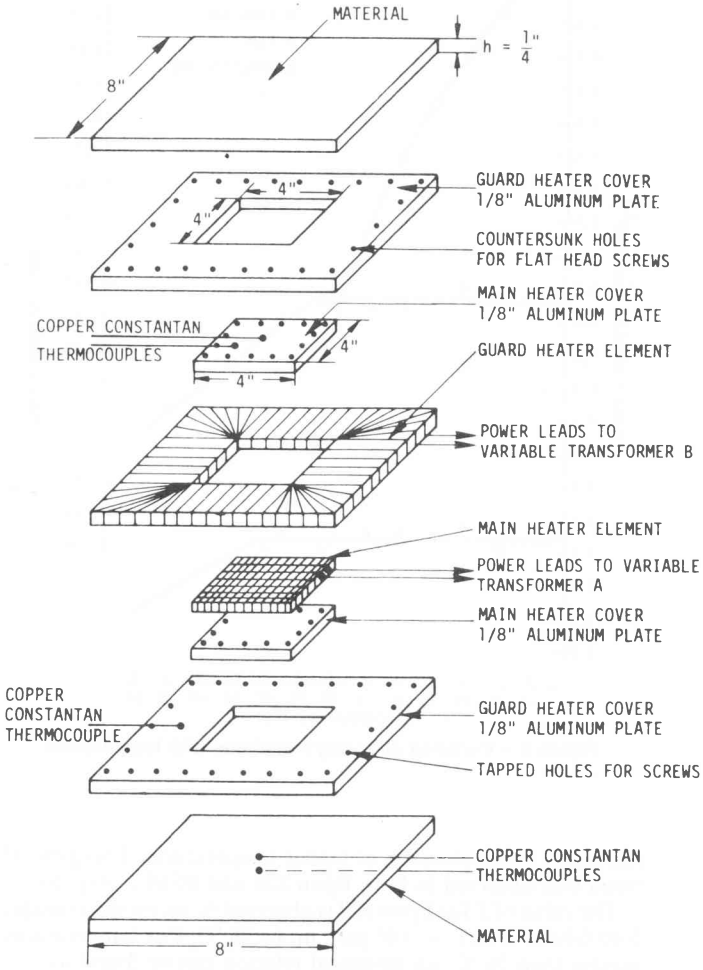


**Figure 4 – Exploded view of guarded-plate assembly for finding *k***

*Materials*

EPON 828 – The basic resin is Shell Chemical Epon 828, 100 parts. The hardener is phthalic anhydride, 50 parts by weight with Shell curing agent Z (1 per cent of total weight).

The curing process for the mixture consists of two cycles. In the primary curing cycle, the material is kept at 93 °C for two hours. Then it is heated at a rate of 8 °C/h to 107 °C and kept at this temperature for two hours. The mixture is then heated up to 116 °C at a rate of 8 °C/h and kept at 116 °C for four hours. Then the material is cooled down to 93 °C at 8 °C/h and removed from the mold. In the postcuring cycle the material is heated up to 124 °C with a gradient of 11 °C/h and kept at 124 °C for four hours. Then it is heated up to 140 °C with a gradient of 8 °C/h and cooled down to 93 °C with a gradient of 4 °C/h. Finally, it is cooled down to room temperature with a gradient of 8-11 °C/h.

PSM-1 – This material is bought in 6.4-mm (0.25-in.) finished sheets from Photolastic, Inc.

ARALDITE 502 – The basic resin is Araldite 502. The hardener is 951 and is cured at room temperature.

## Results

*Young's Modulus*

For two of the materials, Young's modulus did not show much variation at temperatures lower than room temperature. It

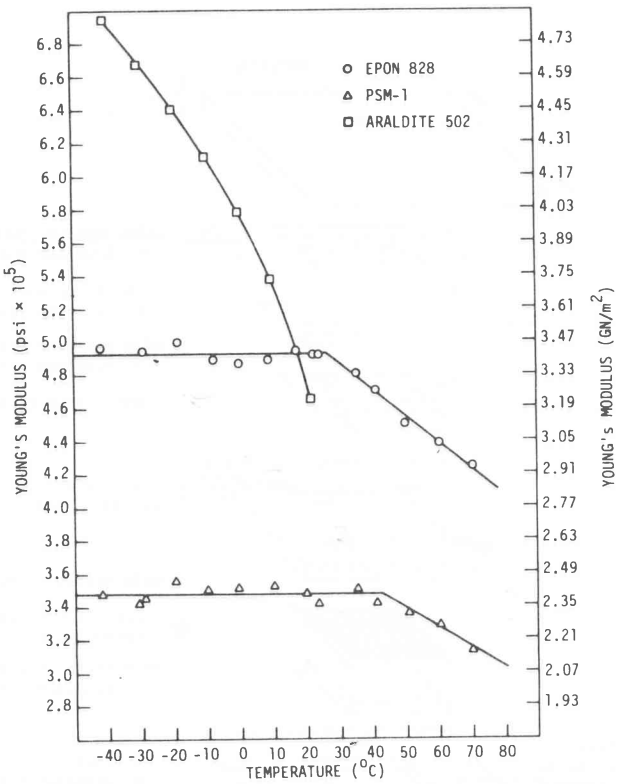


**Figure 5 – Variation of Young's modulus with temperature**

started to drop, however, at higher temperatures. This general trend was observed in both Epon 828 and PSM-1 (Fig. 5).

The value of $E$ for Epon 828 is observed to be, on the average, 3.40 GN/m² (4.93 × $10^5$ psi), up to 26 °C. For temperatures greater than 26 °C, an empirical relation can be found as

$$E = -1.11(10^{-2})T + 3.69 \quad 26\,^{\circ}\text{C} < T < 70\,^{\circ}\text{C} \qquad (9)$$

where $E$ is in GN/m² and $T$ is in °C.

A similar behavior is true for PSM-1 also. The value of $E$ is, on the average, 2.39 GN/m² (3.47 × $10^5$ psi), up to approximately 43 °C; it starts to drop off at temperatures over 43 °C. The empirical relation found for PSM-1 is

$$E = -8.25(10^{-}3)T + 2.74 \quad 43^{\circ}\text{C} < T < 70\,^{\circ}\text{C} \qquad (10)$$

where $E$ is in GN/m² and $T$ is in °C.

Manufacturer's data for $E$ are given as 2.34 GN/m² (3.4 × $10^5$ psi).

On the other hand, Araldite 502 showed a different behavior and the value of Young's modulus decreased monotonically as the temperature was increased, as shown in Fig. 5. A linear regression on the data yielded the equation

$$E = 3.99 - 3.00(10^{-2})T - 2.32(10^{-4})T^2 \quad -40\,^{\circ}\text{C} < T < 22\,^{\circ}\text{C} \qquad (11)$$

where $E$ is in GN/m² and $T$ is in °C.

*Poisson's Ratio*

The Poisson's ratio did not show much variance for a large temperature range for Araldite 502 and PSM-1. For Araldite 502, the value of Poisson's ratio was found to be 0.335 in the interval −40 °C to 22 °C. The variation of $v$ with temperature is shown on Fig. 6. Also, the value of Poisson's ratio was found as 0.383, as opposed to manufacturer's value of 0.38, in the interval −40 °C to 70 °C for PSM-1. This property showed some variance for Epon 828 up to about −10°C and then converged to a constant

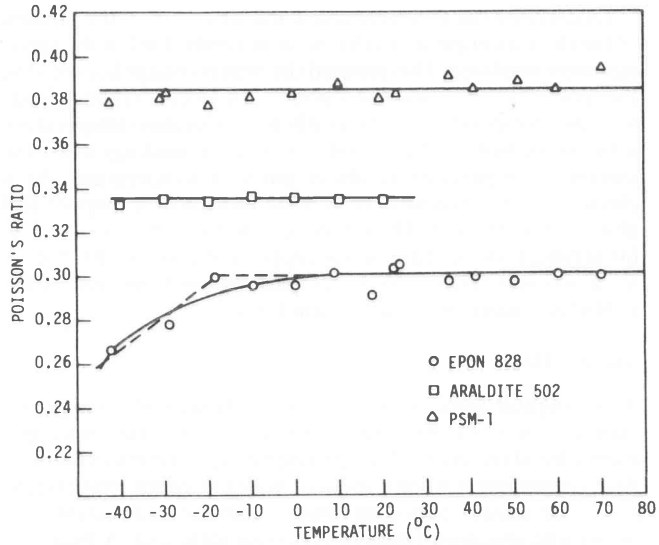


**Figure 6 – Variations of Poisson ratio with temperature**

value of 0.300. For the lower end of the test interval an empirical expression can be found as

$$v = 0.30 + 1.32(10^{-4})T - 7.98(10^{-6})T^2 + 1.36(10^{-7})T^3 - 6.72(10^{-11})T^4 \quad -40\,^{\circ}\text{C} < T < -10\,^{\circ}\text{C} \qquad (12a)$$

where $T$ is in °C.

One may, however, also assume that the Poisson's ratio for Epon 828 behaves as indicated by the dashed lines at the lower end of the test interval. Linear regression considering only the last three points then gives

$$v = \begin{cases} 1.4(10^{-3})T + 0.323 & -40\,^{\circ}\text{C} < T < -22\,^{\circ}\text{C} \\ 0.3 & -22\,^{\circ}\text{C} < T < 70\,^{\circ}\text{C} \end{cases} \qquad (12b)$$

Where $T$ is in °C.

*Stress Birefringence*

The variation of the photoelastic-fringe coefficient with temperature is shown in Fig. 7. The value of $f_\sigma$ for Epon 828 was a constant for the range −40 °C to about 23 °C. It started to drop off with increase in temperature. For the range −40 °C to 23 °C, the value of $f_\sigma$ is 12.1 kN/m (69 lb/in.); and for temperatures higher than 23 °C, a polynomial curve fit yields

$$f_\sigma = 12.18 - 2.92(10^{-4})T^2 - 3.25(10^{-6})T^3 + 4.93(10^{-8})T^4 \quad 23\,^{\circ}\text{C} < T < 70\,^{\circ}\text{C} \qquad (13)$$

where $f_\sigma$ is in kN/m and $T$ is in °C.

PSM-1 and Araldite 502 had constant photoelastic-fringe coefficients. In the interval −40 °C to 60 °C, on the average, the value of $f_\sigma$ for PSM-1 was 7.0 kN/m (40 lb/in.); and in the interval −60 °C to 25 °C, the value of $f_\sigma$ for Araldite 502 was, on the average, 12.7 kN/m (72.5 lb/in.). The value of $f_\sigma$ for PSM-1 is specified as 7.0 kN/m (40 lb/in.) by the manufacturer.

*Coefficient of Thermal Expansion*

The thermal expansion coefficient (Fig. 8) is determined from the slope of the displacement vs. temperature plots. It is observed that between −15 °C and 55 C, there is a linear range for Epon 828. A linear regression on the data in this range yielded

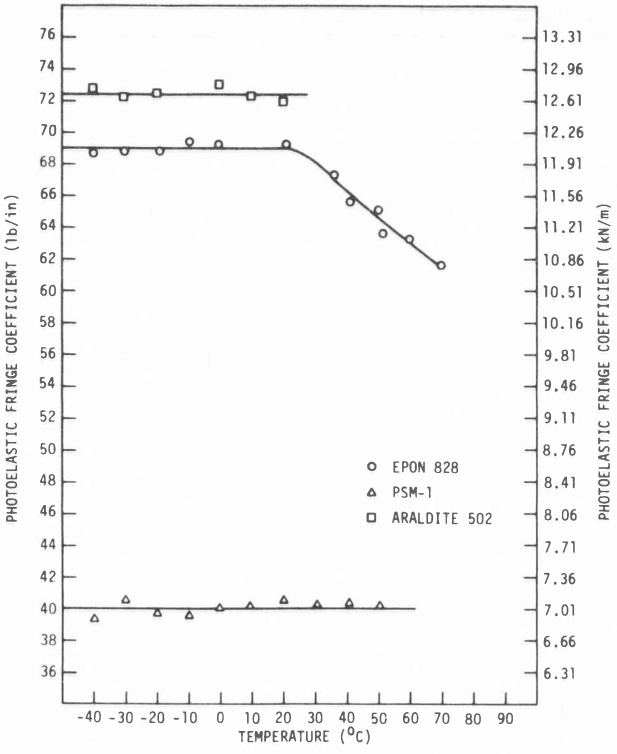


**Figure 7 – Variation of photoelastic-fringe coefficient with temperature**

the coefficient of thermal expansion as $1.36(10^{-4})$ °C$^{-1}$. Similarly, a linear region exists for PSM-1 between −10 °C and 55 °C, and a linear regression yields the value of $\alpha$ as $1.46(10^{-4})$ °C$^{-1}$. The data for Araldite 502 yielded a value for $\alpha$ of $9.5(10^{-5})$ °C$^{-1}$ from −65 °C to −15 °C.

*Specific Heat*

Figure 9 indicates that, for large temperature ranges, the specific heat values are constant for Epon 828 and PSM-1. The range is approximately −50 °C to 93 °C for PSM-1. The slopes of the lines yielded the value of $C_p$ as 0.328 W-h/kg °C (0.282 Btu/lb °F) for Epon 828 and 0.307 W-h/kg °C (0.264 Btu/lb. °F) for PSM-1. Araldite 502 also had a constant specific heat for the temperature range −60 °C to 25 °C. The average value of $C_p$ for this material was 0.325 W-h/kg °C (0.280 Btu/lb °F).

*Thermal Conductivity*

The results show that for the range of −60 °C to 25 °C, the thermal conductivity of Araldite 502 remained constant with a value of 0.204 W/m °C (0.118 Btu/ft-h-°F). Also, Epon 828 and PSM-1 had constant thermal conductivities for this range of temperatures, up to 60 °C. The computed $k$ for Epon 828 was 0.226 W/m °C (0.131 Btu/ft-h-°F) and for PSM-1 it was 0.365 W/m °C (0.211 Btu/ft-h-°F).

Since the thermal conductivities did not show any signicant change in the range of temperatures over which they were measured, no figure is presented for them.

All results are summarized in Table 1.

## Discussions and Conclusions

If the figure of merit is a constant over a temperature range, then the material can be used in thermal-stress modeling in that range. It is observed in Fig. 10 that such a range exists for two of the three materials tested. In the interval −15 °C to 55 °C, Epon 828 has a constant $Q_t = 38.27$ m$^{-1}$ °C$^{-1}$ (0.972 in.$^{-1}$ °C$^{-1}$); and in the interval −10 °C to 55 °C, PSM-1 has constant $Q_t$ of 49.61 m$^{-1}$ °C$^{-1}$ (1.26 in.$^{-1}$ °C$^{-1}$). Araldite 502 did not exhibit such a behavior and the $Q$ vs. $T$ relationship can be approximated by the straight line

$$Q_t = -169T + 30.16 \qquad (14)$$

where $Q_t$ is in m$^{-1}$ °C$^{-1}$ and $T$ is in °C.

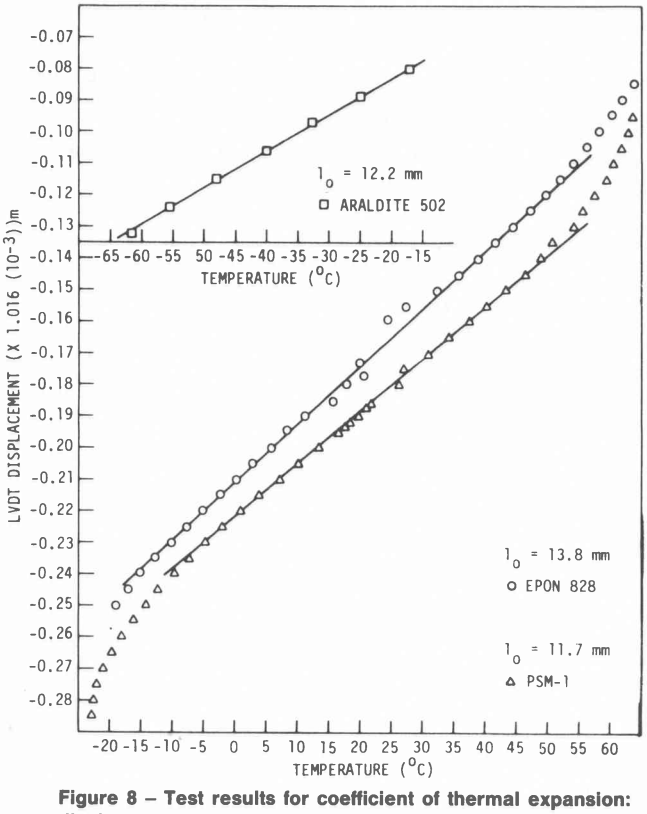


**Figure 8 – Test results for coefficient of thermal expansion: displacement vs. temperature plots from LVDT measurements**

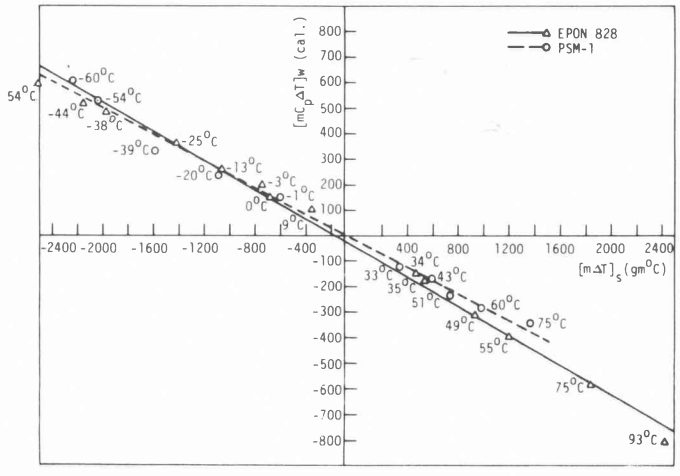


**Figure 9 – Nondimensional plot for specific heat. Subscripts *w* for water and *S* for specimen**

**TABLE 1 — SUMMARY OF THE MATERIAL PROPERTIES FOR THE MODEL MATERIALS EPON 828, PSM-1, ARALDITE 502**

| | | Epon 828 | | PSM-1 | | Araldite 502 | | |
|---|---|---|---|---|---|---|---|---|
| | Units | Value | T(°C) | Value | T(°C) | Value | T(°C) | Figure |
| $E$ | GN/m² | 3.40 | −40 to 26 | 2.39 | −40 to 43 | | | 5 |
| | psi | 4.93(10⁵) | | 3.47(10⁵) | | | | |
| | | eq (9) | > 26 | eq (10) | > 43 | eq (11) | < 22 | |
| $\nu$ | — | 0.3 | > −10 | 0.38 | −40 to 70 | 0.34 | −40 to 22 | 6 |
| | — | eq (12a) | −40 to −10 | | | | | |
| $f_\sigma$ | kN/M | 12.1 | −40 to 23 | 7.0 | −40 to 60 | 12.7 | −60 to 25 | 7 |
| | lb/in. | 69.0 | | 40.0 | | 72.5 | | |
| | | eq (13) | > 23 | | | | | |
| $\alpha$ | °C⁻¹ | 1.36(10⁻⁴) | −15 to 55 | 1.46(10⁻⁴) | −10 to 55 | 9.5(10⁻⁵) | −60 to −15 | 8 |
| $C_p$ | W-h/kg °C | 0.328 | −50 to 93 | 0.307 | −50 to 75 | 0.325 | −60 to 25 | 9 |
| | Btu/lb °F | 0.282 | | 0.264 | | 0.280 | | |
| $k$ | W/m °C | 0.227 | | 0.365 | | 0.204 | −60 to 25 | |
| | Btu/ft-h-°C | 0.131 | | 0.211 | | 0.118 | | |
| $\varrho$ | kg/m³ | 1250 | | 1170 | | 1300 | | |
| | lb/ft³ | 78.0 | | 73.0 | | 81.2 | | |
| $\beta$ | m²/h | 5.54(10⁻⁴) | | 1.01(10⁻³) | | 4.82(10⁻⁴) | | |
| | ft²/h | 5.96(10⁻³) | | 1.09(10⁻²) | | 5.19(10⁻³) | | |
| $Q_t$ | fr/m °C | 38.27 | −15 to 55 | 46.61 | −10 to 55 | eq (14) | −40 to 20 | 10 |
| | fr/in. °C | 0.972 | | 1.26 | | | | |

Another parameter which is of importance in transient analysis is the diffusivity, $\beta$. Since the magnitude of the stresses developed due to transient-temperature gradients will be proportional to the diffusivity, a photoelastic material with a higher $\beta$ will be preferred for transient-thermal-stress analysis.

In conclusion, PSM-1 and Epon 828 can readily be utilized for transient-thermal-stress analysis. Since $Q_t$ is constant over a reasonable temperature range above room temperature, it is not necessary to use the refrigeration technique[2,3]. This eliminates much of the experimental difficulties and makes transient-thermal-stress modeling much more repeatable, cheaper to perform, and ultimately more reliable. PSM-1 emerges as the best photothermo-elastic material in the group.

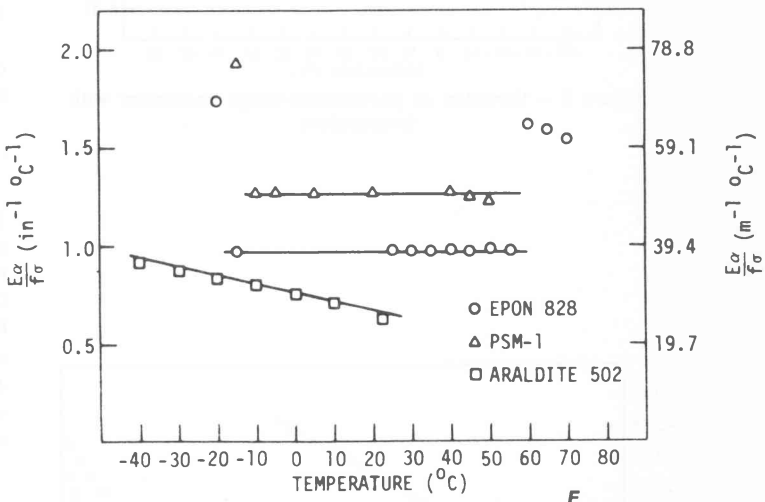


**Figure 10 – Variation of figure of merit, $Q_t = \frac{E_a}{f_\sigma}$, with temperature**

*Acknowledgments*

This experimental program was supported by the Department of Engineering Science and Mechanics and the Engineering Research Institute of Iowa State University.

## References

1. Hovanesian, J. D. and Kowalski, H. C., "Similarity in Thermo-elasticity," *Experimental Mechanics*, 7 (2), 82-84 (1967).

2. Burger, C. P., "Thermal Modeling," *Experimental Mechanics, 15* (11), 430-441 (1975).

3. Burger, C. P., "A Generalized Method for Photoelastic Studies of Transient Thermal Stresses," *Experimental Mechanics, 9* (12), 529-537 (1969).

4. Tsuji, M. and Oda, M., "investigation of Photothermoelasticity by Means of Heating," J. of Thermal Stresses, **2,** 215-232 (1979).

5. Marloff, R. H., "Thermal Tests of a Steam-turbine Nozzle-chamber Model," *Experimental Mechanics, 19* (11), 399-405 (1979).

6. ASTM Standard, Part 3, 1084 (1955).

Gedruk en gebind deur
Nasionale Boekdrukkery
Goodwood, Kaap.